CHAPTER

Lab-on-a-chip (lab-on-a-phone) for analysis of blood and diagnosis of blood diseases

11

Fahima Akther[1,2], Huong D.N. Tran[1,2], Jun Zhang[2], Nam-Trung Nguyen[2] and Hang T. Ta[1,2,3]

[1]Australian Institute for Bioengineering and Nanotechnology, University of Queensland, St Lucia, QLD, Australia
[2]Queensland Micro- and Nanotechnology, Griffith University, Nathan, QLD, Australia [3]School of Environment and Science, Griffith University, Nathan, QLD, Australia

11.1 Introduction

Human whole blood is a major biofluid because it carries the key physiological and pathological information (Kuan & Huang, 2020). Blood mainly consists of blood cells such as red blood cells (RBCs), white blood cells (WBCs), platelets, and plasma. Under normal conditions, each component exhibits distinct physiological properties, including size and the total number of blood cells, and the concentration of different blood proteins (Kuan & Huang, 2020). The quantity of various molecular components present in the blood, including proteins, nucleic acids, and metabolites, can be used as diagnostic parameters for many diseases (Liu et al., 2019). Deviation from the normal parameters can be linked to a specific disease condition. A blood test could provide a rapid and precise diagnostic platform by analyzing different circulating biomarkers. A conventional blood test requires multiple steps such as mixing, lysing, centrifugation, and filtration for accurate and sensitive detecting of the biomarkers (Lee et al., 2019). Furthermore, the process requires bulky and expensive laboratory equipment operated by skilled personnel, which increases the cost of the test. Therefore conventional analyzers usually use a considerably large amount of blood that prolongs the data acquisition time, typically from 1 day to several days (Kuan & Huang, 2020; Mabey et al., 2004), limiting the capability of point-of-care (POC) diagnosis in emergencies. As a result, extensive investigations are conducted to develop easy, efficient, and rapid POC diagnostic tools that can be operated at the patient site with minimum skills (Arshavsky-Graham & Segal, 2020).

To address this issue, miniaturized lab-on-a-chip (LOC) devices have been becoming popular for blood analysis. LOC devices must function without bulky infrastructure, as well as independent of location for direct use in POC treatment (Emde et al., 2020). Recent advancement in microfluidic technology plays a vital role in handling and processing of a small amount of liquid, and the integration of small biosensors in the LOC devices for real-time observation (Mach et al., 2013). More importantly, microfluidic LOC devices significantly reduce the sample and reagent volume, and shorten analyzing time with higher accuracy and reproducibility (Li, 2005). For instance, Kuan et al. (2016) reported a microfluidic device that was able to process whole blood and detect Hgb (Hemoglobin) and HbA1c (glycated hemoglobin) within 30 minutes by using only 5 μL of blood,

Nanotechnology for Hematology, Blood Transfusion, and Artificial Blood. DOI: https://doi.org/10.1016/B978-0-12-823971-1.00009-X

which corresponds to a 300-fold reduction from the required volume for a standard analyzer. On the other hand, a thermoplastic chip could detect ABO/Rh blood typing within a minute using just 1 μL of blood sample via colorimetric detection (Chen et al., 2015). Huet et al. (2017) designed an automated passive microfluidic biochip that was able to detect the real-time positive and negative agglutination of RBCs in less than 2 minutes with 100% accuracy. Furthermore, the integration of the smartphone with the microfluidic LOC devices gradually shifts the diagnosis platform from centralized laboratories to individual homes driven monitoring (Liu et al., 2019). Smartphone's features such as a high-resolution camera, in-built apps, and computational units can be integrated with other analytical sensing systems to produce highly sensitive medical testing (Arshavsky-Graham & Segal; Liu et al., 2019). Low cost, simple operation technique, and portability make smartphone-based LOC devices a good alternative in resource-limited areas. In addition, smartphone apps allow the storage of data in a database or the wireless transmission of data to remote sites (Lee et al., 2020; Romeo et al., 2016).

This chapter provides a concise overview of recent development of LOC devices for whole blood analysis. We mainly discuss the fabrication techniques and the working principle of the chips for blood cell separation, blood typing, and disease diagnosis in POC platforms. This chapter also discusses the widely applied sensing modalities for analyzing blood diseases in smartphone-based LOC devices. Here, we highlight the detection principles for each sensing technique with several relevant examples. Finally, we discuss the main challenges and promising prospects in this field. A graphical overview of this chapter is presented in Fig. 11.1.

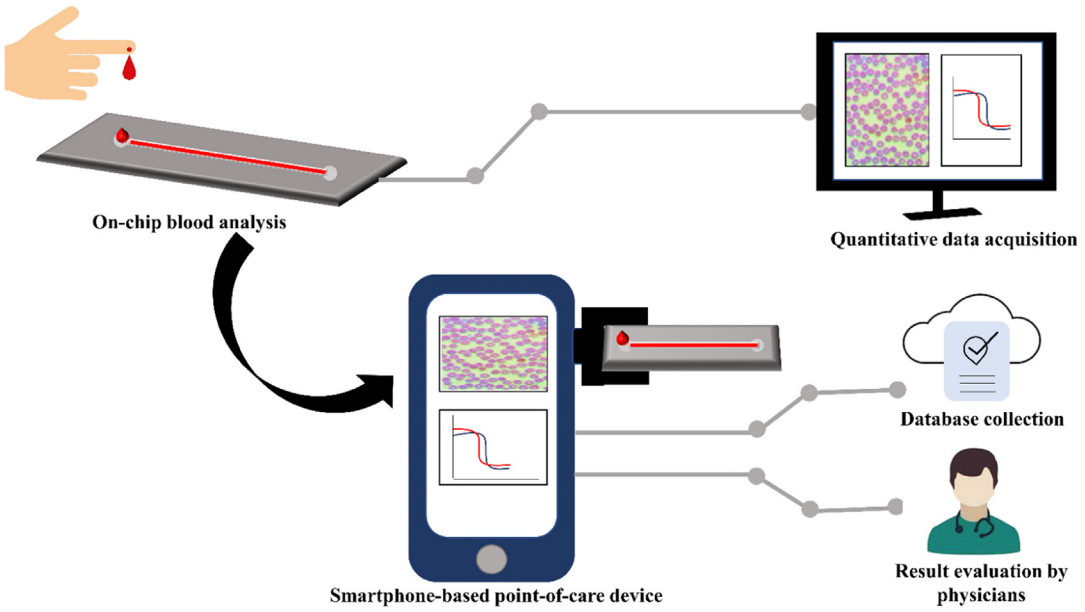

FIGURE 11.1

Schematic representation of the uses of lab-on-a-chip (LOC) devices for point-of-care blood analysis and the modulation of smartphone technologies with LOC devices for on-site or remote data analysis.

11.2 On-chip whole blood analysis and disease diagnosis

Blood is a widely used biological sample for regular clinical analysis. Blood components carry critical physiological and pathological information of the human body. Quantification of cellular components of blood is commonly required for disease identification and management. For example, a complete blood count (CBC) provides an overall health status of a patient by monitoring the shape, size, and the number of each cell type, as well as the concentration of different proteins or metabolites in the blood (Kuan et al., 2018). This sophisticated test requires expensive automated hematology analyzers and flow cytometers for precise data acquisition. Moreover, conventional techniques require a large volume of blood ($\sim$1 mL) and trained staff for handling, which restrain the blood analysis in POC settings (Kuan et al., 2018). LOC technology is emerging as a miniaturized point-of-care diagnostic platform for disease diagnosis from a single drop of blood. Due to the advanced control over fluid behavior (Nikoleli et al., 2018), microfluidic LOC technology has superior advantages such as the reduction of sample and reagent volume, rapid responses, shorter analysis time, along with the cut down of cost per test (Lee et al., 2019; Nikoleli et al., 2018). This section provides an overview of LOC devices for the analysis of blood components and blood diseases. Table 11.1 lists a summary of the characteristic features of the LOC devices for analyzing human whole blood.

11.2.1 On-chip separation of blood components

Whole blood is a mixture of different components, and each has its unique attributes. Analyzing the blood components is a key diagnostic step where the accurate separation of the blood components plays a critical role in the precision of a specific test. In order to design a successful LOC blood analyzer, some characteristic attributes should be considered. For instance, the LOC-based devices must show sufficient sensitivity to the microscale blood sample. Also, the design should facilitate the incorporation of the on-chip sensor for the separation of blood components, rapid detection and communication of the signals, and translation of the signals into a readable clinical outcome (Lee & Lee, 2013). Recent studies mainly focus on developing simple LOC devices for whole blood processing in a single chip (Dixon et al., 2020; Kim et al., 2019; Kuan et al., 2018; Lee et al., 2019; Li et al., 2013; Madadi et al., 2015; Nguyen et al., 2015; Yang et al., 2019). Furthermore, LOC devices can process whole blood without any external instrument such as a centrifuge (Kuan & Huang, 2020). Kuan et al. (2018) designed a multichannel PDMS (polydimethylsiloxane) device for simultaneous processing of plasma, RBCs, and WBCs in a single device without any interference. The chip consisted of a separated whole blood inlet, a buffer inlet, and a bifurcation zone. The bifurcation zone contained 10 side channels and one main channel. Six bead-packed (10 μm beads) side channels were used for plasma extraction, while four-necked side channels (2 μm neck) and the main channel were used to trap RBCs and WBCs, respectively. All side channels were positioned at 60-degree angles with the main channel to maintain the uniform flow throughout the device. The unique chip design separated the blood components by following the bifurcation law and crossflow method. According to the bifurcation law or Zweifach-Fung effect, at the bifurcation point of the microvascular network, the daughter channels with the high flow velocity tend to pull the higher fraction of the RBCs (Mantegazza et al., 2020). When the blood and the

Table 11.1 A summary of the characteristic features of the lab-on-a-chip devices used in blood analysis.

Application	Chip design	Mechanism	Injected sample	Required time	Required sample volume	Target	Results	References
Analyzing whole blood, including plasma and RBCs (red blood cells) extraction, and WBCs (white blood cells) trapping.	– A PDMS (polydimethylsiloxane) chip consisted of a separated whole blood inlet, a buffer inlet, and a bifurcation zone. – The bifurcation zone contained ten side channels and one main channel. – Six bead-packed (10 μm-bead) side channels were used for plasma extraction, while four-necked side channels (2 μm-necked) and the main channel were used for trapping the RBCs and WBCs, respectively.	Bifurcation law and crossflow method.	Whole blood	20 min	6 μL	– Plasma – RBCs – WBCs	– Plasma extracted by the microfluidic device had a minimum dilution factor (0.76X) and low hemolysis effect. – Extracted RBCs could use for blood typing. – Up to ~1800 WBCs could be trapped in 20 min.	Kuan et al. (2018)
Measurement of whole blood viscosity, hematocrit, and RBCs deformability	– The chip consisted of two parts: microviscometer and microhemocytometer. – The microviscometer was molded from PDMS and the electronic components for the hemocytometer was made of a printed circuit board. – Microviscometer had 10 arrays, each of which had 100 microchannels.	– Viscosity was measured by the fluid distribution according to the hydraulic resistances from the given equation: $R = \frac{12\mu L}{wh^3 N}\left(1 - \frac{192h}{\pi^5 w}\sum_{n=1,3,5,\ldots}\frac{1}{n^5}\tanh\left(n\pi w/2h\right)\right)^{-1}$ where, R, μ, L, w, h, and N denote the hydraulic resistance, viscosity, channel length, width, height, and number of channels filled with fluids, respectively. – Hematocrit was estimated from the electrical characteristic of the blood cytoplasmic resistant, and plasma resistant, while RBC deformation was detected from the change of membrane capacitance.	– Whole blood – Chemically hardened RBC with plasma	~5 min	500 μL	– Whole blood – RBCs	– The normalized difference for the whole blood viscosity measurement by the physiometer was 0.8% ± 1.4% less than the values obtained from the rotational cone-and-plate viscometer. – For hematocrit measurement, physiometer showed lower coefficient of variance (0.3%–1.2%) than the centrifuge (2.0%–2.7%). – For RBCs deformability measurement, a strong linear correlation ($R^2 = 0.97$) was observed between the deformability index acquired from physiometer and estimated from the image acquisition.	Kim et al. (2019)

– Blood/ plasma separation	– The simple chip design with a main channel (5 mm long and – 240 μm wide) and a side channel (1 mm long and 120 μm) was manufactured by suing lamination-based microfabrication. – Optically transparent indium tin oxide coated glass was used to form electrodes and underlying substrate.	This dielectrophoresis (DEP)-based microfluidic device continually extracted the plasma by generating nonuniform electric field with a higher gradient at the junction area.	– Whole blood	~7 μL	15 min	Plasma	– The purity of the extracted plasma by the DEP plasma extractor was close to 100% with a yield of approximately 31%.	Yang et al. (2019)
Blood/plasma separation	– The digital microfluidic (DMF) device consisted of two plates: inkjet-printed bottom plate (black outline) and ITO (indium tin oxide)-PET top plate – The top plates were formed from ITO-PET substrates coated with FluoroPel PFC 1101 V as – The bottom plate consisted of 77 roughly square interdigitated driving electrodes (2.8 × 2.8 mm), 8 reservoir electrodes (7.6 × 6.4 mm), and 8 dispensing electrodes (5.6 × 2.0 mm). – Three integrated porous membranes with the bottom plate: plasma separation membrane for trapping RBCs, transport membrane for delivery of filtered plasma into electrode array, and impregnated wax plug to limit the flow of plasma in the TM.	Membrane filtration method.	– Whole blood	~50 μL	4 min	Plasma	The device performance was compared with the standard centrifugation technique and no cell was observed in extracted plasma under microscope which indicated almost 100% purity of the plasma.	Dixon et al. (2020)
Blood Typing	– A single-channel microfluidic chip was fabricated by using cyclic olefin polymer (COP). – The channel was embedded with dried anti-An or anti-B dried reagents.	Passive fluid flow	Undiluted or diluted blood with PBS (phosphate buffer saline) (1:5)	6.5 μL	Less than 10 min for undiluted blood and 100 s for diluted blood	Agglutination of RBCs	The embedded reagents triggered the agglutination reaction and exhibited 100% accuracy in identifying ABO blood typing.	Huet et al. (2018)

(*Continued*)

Table 11.1 A summary of the characteristic features of the lab-on-a-chip devices used in blood analysis. *Continued*

Application	Chip design	Mechanism	Injected sample	Required time	Required sample volume	Target	Results	References
– Blood/ plasma separation – Blood typing	The device consisted of a PDMS main channel for the blood transportation, a top plasma collector channels, and a bottom etched glass that has the array of pillars for plasma extraction.	Cell separation from the plasma was done by applying the hydrodynamic forces.	– Whole blood – IgM antibodies.	50 μL	10 min	– Plasma – Agglutination of RBCs	– The device could successfully yield a 12% of plasma with 100% purity. – The ABO/Rh grouping was successfully done by observing the agglutination in both antigens of RBCs (forward) and antibodies of plasma (reverse) via naked eyes and microscopic images. – The device could not detect the agglutination in highly viscous sample containing hematocrit higher than 50% but for hematocrit lower than that the results showed an agreement for all 4 types of blood.	Karimi et al. (2019)
Blood typing	Long-range surface plasmon resonance (LR-SPR) was consisted of high refractive index glass, Cytop film layer, and thin gold film. – The anti-A or anti-B was covalently immobilized on the gold surface.	– This LR-SPR based device worked by observing change in refractive index.	– RBC-An and RBC-B samples – Anti-An and Anti-B monoclonal antibody	The lowest detection limits were 1.58×10^5 cells/mL for RBC-An and 3.83×10^5 cells/mL for RBC-B.	10 min	RBC	– The results of the ABO blood typing produced by the LR-SPR based chip were consistent with those obtained from the gold standard test of agglutination. – The LR-SPR chip showed higher sensitivity compared to the Short-range SPR devices.	Tangkawsakul et al. (2016)
Blood typing	A surface plasmon resonance (SPR) array coupled with multiple anti-RBC antibodies was designed and placed in a flow chamber for multiplex blood typing.	The blood samples ran through the flow chamber and blood typing was determined by monitoring RBC-antibody binding on the SPR array.	– Diluted whole blood in PBS (120-fold dilution). – IgM and IgG antibodies.	200 μL	5 min	RBC	– The chip was reusable and could use to test at least 100 samples. – The ABO/Rh typing results gave 100% match with the results obtained from classical serology with all antibody except anti-E/e monoclonals	Szittner et al. (2019)

– Blood typing – Cross matching	– The PDMS device consisted of a dilutor, a homogenizer, and four detectors. – The dilutor was divided into three inlets for whole blood, PBS, and air, a T-shaped and a Y-shaped junction.	– The dilution was performed by applying a microbubble motion. – Preloaded blood typing reagents were remained stand by in the reaction chamber and blood typing was determined by the RBCs-specific antibody reaction. – Crossmatch was done by mixing RBCs with serum.	– Dilution of the blood with PBS was done automatically inside the device. – Anti-A, anti-B, and – anti-D reagents	350−500 μL	~5 min	RBC	– Nonuniformity of the mixing of blood-PBS was notices at the end of the mixing channel because of the low flow disturbance created from the microbubbles. – The device exhibited high sensitivity to detect weak agglutinations even at level 1 + without any illumination. – No data was available for cross-matching.	Yamamoto et al. (2020)
– Blood/ plasma separation – Blood cross-matching	– The device consisted of three PDMS layers (3 mm thickness), one thin PDMS membrane layer (25 μm thickness), and two plasma separation membranes connected with a pressure chamber.	– Donor and recipients' blood were injected to the chip via two inlet and then separated individual's plasma through the two plasma separation membranes. – The cross-matching results were achieved by cross-reacting the donor's blood plasma with the recipient's whole blood (minor test) or recipient's blood plasma with the donor's whole blood (major test) by pushing and releasing the pressure chamber.	Whole blood	50 μL	10 min	– Plasma – RBC	– The transfusion suitability was interpreted depended on the degree of agglutination. 1. Compatible when agglutination did not occur in both major and minor test. 2. Incompatible when agglutination occurred in the major test but not in the minor test. 3. Incompatible when agglutination occurred in the minor test but not in the major test, but a little amount of blood could be transfused in emergencies. 4. Completely incompatible if agglutination occurred in both major and minor test.	Park and Park (2018)
Disease diagnosis-Anemia	– The paper-based microfluidic colorimetric chip was fabricated on Whatman (Grade-1) cellulose filter paper with the mean pore of 11 μm by inkjet printing. – A hydrophilic reaction pads for colorimetric detection was attached to guide the fluid flow through the porous network.	– Hemoglobin (Hgb) was detected from the redox reaction between 3,3′-Dimethyl- [1,1′-biphenyl]-4,4′-diamine (o-tolidine) and hydrogen peroxide yielding greenish-blue colored oxidized o-tolidine products – The Hgb concentration was estimated from the colorimetric signal intensity.	– Whole blood – Drabkin's solution	2 μL	2.5−3.5 min	Hgb concentration	– The results obtained from the colorimetric device showed strong correlation with the standard hematology analyzer ($r = 0.909$), – The device showed 87.5%, and 100% sensitivity for detecting mild, and severe anemia, respectively with 100% specificity in both cases. – The color-scale yielded quantitative measurement within 1.5 g/dL Hgb	Biswas et al. (2018)

(*Continued*)

Table 11.1 A summary of the characteristic features of the lab-on-a-chip devices used in blood analysis. *Continued*

Application	Chip design	Mechanism	Injected sample	Required time	Required sample volume	Target	Results	References
							concentration for 91% sample.	
Disease diagnosis-Anemia	– A rectangular microfluidic channel with a length, width, and height of 3 cm × 200 × 50 μm was fabricated by using PDMS. – A miniature microscope was designed to measure the intensity of the transmitted light.	Hemoglobin level was optically detected from whole blood without hemolysis by illuminating the blood in a microfluidic channel at a peak wavelength of 540 nm. – The absorbance of the samples was measured by using a CMOS sensor coupled with a lens to magnify the image onto the detector.	Diluted blood with calcium free Tyrode buffer	–	–	Hgb	– The device could measure Hgb concentration approximately 3.20 g/dL, 4 g/dL, and 5.5 g/dL for severe, moderate, mild cases of anemia, successively. – The device was enabled to detect the optical density for the flowing blood at a shear rate of 500 s^{-1}.	Taparia et al. (2017)
Disease diagnosis-Anemia	On-wafer based device was fabricated by silicon wafer and connected to computer interfaced software controlled electronic circuit.	The electrical parameters of the erythrocyte suspensions with varying levels of hematocrit were obtained by impedance/capacitance spectroscopy and current-voltage (I-V) measurement.	Diluted blood with PBS	20 μL	<3 s	Hematocrit	– The detection limit for the hematocrit measurement was 3.5%. – The impedance value increased with increase hematocrit level while reduction was observed in capacitance values. – The device was highly sensitive and could detect the change in capacitance and impedance with the variation of the hematocrit level by 1%.	Chakraborty et al. (2020)
Disease diagnosis-Acute promyelocyte leukemia	– The microfluidic chip consisted of eight parallel microfluidic channels with separated inlets and outlets. – A chip holder was used to connect the tubes with the chip. – The quantity of the liquid flow through all channels could	– In bead-based sandwich ELISA, anti-PML-biotin antibody was used as capture antibody and the anti-RAR_-HRP (horseradish peroxidase) antibody as detection antibody. – The detection mechanism was followed by several	– NB-4, HL-60 and MV4−11 cell lines – Five primary patient samples: Three FAB (French−American−British classification system) type M3 samples and one FAB type M4 and one M5 (PML-RAR_-negative samples). – PBS	– The assay solution contained l 10−0.1 μg total cell lysate and 0.1 μg protein from patient's sample.	~1 h	PML-RAR fusion protein	– The result suggested the fluorescence intensity of the positive signals was at least 20 times higher than the negative signals. – The chip was sensitive at very low concentration of fusion protein and was able to detect	Emde et al. (2020)

	maintain via a sample loop in the three-way valve, where flow could control individually through all channels by using a motor selection valve.	steps: 1. the PML-RARα expression in cells was shown with subsequent cell lysis outside the chip. 2. The cell lysate was then incubated with the sandwich ELISA in the microfluidic chip. 3. The PML region of the fusion protein was bound with the anti-PML antibody, while RAR_ region was bound with the anti-RAR_-HRP antibody. 4. The reduction reaction of the fusion protein was catalyzed by HRP and converted resazurine to resorufine which was determined by measuring fluorescence intensity.					from 5 ng/μL concentration. – The device required 98.5% less assay components than the conventional systems.	
Disease diagnosis-Leukemia	– The microfluidic PDMS device was consisted of a prefilter region and a single cell trapping region. – Prefilter section was constructed as pillar with a pitch of 25 μm. – The device had 16 parallel trapping channels.	– Size based cell separation via single-cell trapping array was done by passive hydrodynamic forces. – Identification of leukemia cell was done by analyzing phasor-FLIM (fluorescence lifetime imaging microscopy) imaging of the single cell.	Diluted blood with PBS	A large volume of sample could continuously use to trap the single cell.	3 min	– Leukemia cells- THP-1, Jurkat and K562 cells, – WBCs	– The trapping efficacy of WBC and leukemia cells was 78%. – Different leukemia cell lines were quantitatively differentiated from each other with AUC (area under curve) values higher than 0.95, which indicating high sensitivity and specificity for single cell analysis. – When 2% hematocrit sample was running through the device the rate of 0.2 mL/h, ~72,000 single leukemia cells and WBCs could be trapped in 6 min.	Lee et al. (2018)

(*Continued*)

Table 11.1 A summary of the characteristic features of the lab-on-a-chip devices used in blood analysis. *Continued*

Application	Chip design	Mechanism	Injected sample	Required time	Required sample volume	Target	Results	References
Disease diagnosis-Acute lymphoblastic Leukemia	A herringbone straight channel was fabricated by using PDMS and coated the surface with capture antibodies.	The device separated peripheral blood lymphoblasts by using affinity separations technique.	Lymphoblasts spiked in blood	–	30 min	Lymphoblast	The device isolated CCRF-CEM lymphoblasts, patient-derived lymphoblast COG-LL332, and COG-LL317 cell lines with 82%−97%, 80%−97%, and 57%−92% purity, respectively with the initial spike concentrations of <1%.	Li et al. (2017)
Disease diagnosis-Multiple myeloma (MM)	The PDMS chip consisted of a sample prefilter region with multiple layers of micropillars and a cell capture region with 8 separate channels.	Cell sorting was based on the difference between clonal plasma cell and blood cell physical properties such as deformability, size, hydrodynamic properties through some microstructural units in the chip.	Human myeloma cancer cell lines spiked in healthy donor blood	– 1 mL for myeloma cell spiked blood. – 0.5 mL for patient's blood.	More than 4 h at the flow rate of 0.5 mL/h for 1 mL.	Clonal plasma cell	– The chip was able to filter out 99.99% of WBCs. – The capture efficacy of the device for clonal plasma cells from the myeloma cell spiked blood was approximately 40%−55%. – The device was enabled to isolate clonal plasma cell from MM relapsing patients and 117 cells were captures from 0.5 mL of blood while no cell was captured from the healthy donor.	Ouyang et al. (2019)
Disease diagnosis-Plasma cell disorders (PCDs) including monoclonal gammopathy of undetermined significance (MGUS), smoldering multiple myeloma (SMM), and multiple myeloma (MM).	– The device consisted of 50 sinusoidal channels with dimensions of 25 μm (width) and 150 μm (depth), fabricated in COC polymer using hot embossing and arranged in a Z-configuration. – The surface of the channels was modified with covalently attached anti-CD138 antibodies for selecting clonal plasma cells that expressed CD138.	– The device was designed to isolate the circulating clonal plasma cells via positive affinity selection from the whole blood. – To check the device efficacy, approximately ∼ 500 RPMI-8226 cells were seeded into the whole blood from healthy donors (1 mL).	– Patient's whole blood – RPMI-8226 cell	1 mL of whole blood	1 mL of whole blood can be processed in ∼1 h	Clonal plasma cells	– The device showed high sensitivity for isolating clonal plasma cells directly from the patient's blood even those with MUGS, while the higher cell burden was noticed in the patients with symptomatic MM. – Approximately 69% RPMI-8226 cells recovery was achieved by this device.	Kamande et al. (2018)

PBS (phosphate buffer saline) were introduced through the blood and buffer inlets, respectively, a boundary or a crossover layer between the two fluids was formed. The flow rate ratio between the whole blood and the PBS was 1:10, which pushed the cells onto the wall of the blood inlet and directed towards the bifurcation region. Because of the small pore size of 1.55 μm of the bead-packed channels, only blood plasma could flow through these channels. On the other hand, due to the smaller size and higher deformability, RBCs could squeeze through the 2 μm-necked channels. Only the bigger size WBCs traveled to the main channel and retained in the trapping unit. The dilution factor of the acquired plasma was checked by measuring the absorbance to confirm the quality of the plasma for further biomarker detection. The results demonstrated successful plasma extraction with a minimum dilution factor of 0.76×. The hemolysis effect and the intensity profile of the extracted plasma from the chip were similar to that from the standard centrifugation. Extracted RBCs were directly checked using blood typing, demonstrating the extraction of fully functional RBCs from the device. Utilizing the geometry of the trapping units, the device was able to trap up to ~1800 WBCs in 20 minutes from 6 μL of blood.

A cyclic olefin copolymer (COC)-based LOC device was developed for blood/plasma separation via asymmetric capillary force on the POC platform. The main advantage of this design was that the lateral transportation of whole blood by capillary pumping without any external power. The detection was done by a capillary-driven lateral flow colorimetric assay. Another simple dielectrophoresis-based microfluidic device was designed to separate human plasma without any dilution to minimize the potential error of the traditional plasma separator (Yang et al., 2019). The chip design was straightforward with the main channel and a side channel (Fig. 11.2A). At the bottom surface of the chip, two thin electrodes were positioned perpendicularly to the main channel and parallel to each other, which generated the nonuniform electric field with a higher gradient on the junction area. When blood was infused through the main channel, the blood cells experienced a strong negative dielectrophoresis force against the hydrodynamic force that repelled the cells from the flow direction and directed them towards the side channels. The chip was completely optically transparent, allowing for real-time visualization of plasma separation under a microscope. Most importantly, the purity of the extracted plasma was almost 100% with a yield of approximately 31%.

Moreover, a microfluidic-based physiometer, equipped with a temperature controller, was designed to study the blood viscosity, hematocrit level, and RBCs deformability on a chip (Kim et al., 2019). The physiometer consisted of two main parts: a PDMS molded microviscometer and an electronic printed circuit board that worked as a microhemocytometer. The microviscometer was composed of 10 arrays, and each array had 100 microchannels. The results obtained from the device showed a strong correlation with the corresponding gold standard methods. The viscosity measured by the physiometer only showed 0.8% ± 1.4% differences with the rotational cone-and-plate viscometer. The coefficient of variation for hematocrit measurement was 0.3%−1.2% less for the physiometer than the result obtained from centrifugation. Also, measuring the deformability index using a physiometer and standard image processing exhibited a strong coefficient of determination of 0.97.

However, plasma separation from a finger-prick volume of blood remains an enduring challenge for the POC platform (Kersaudy-Kerhoas & Sollier, 2013). Dixon et al. (2020) proposed a digital-based portable microfluidic device to overcome this limitation. Their design had an integrated porous membrane for automated plasma separation. The chip was able to perform the complex,

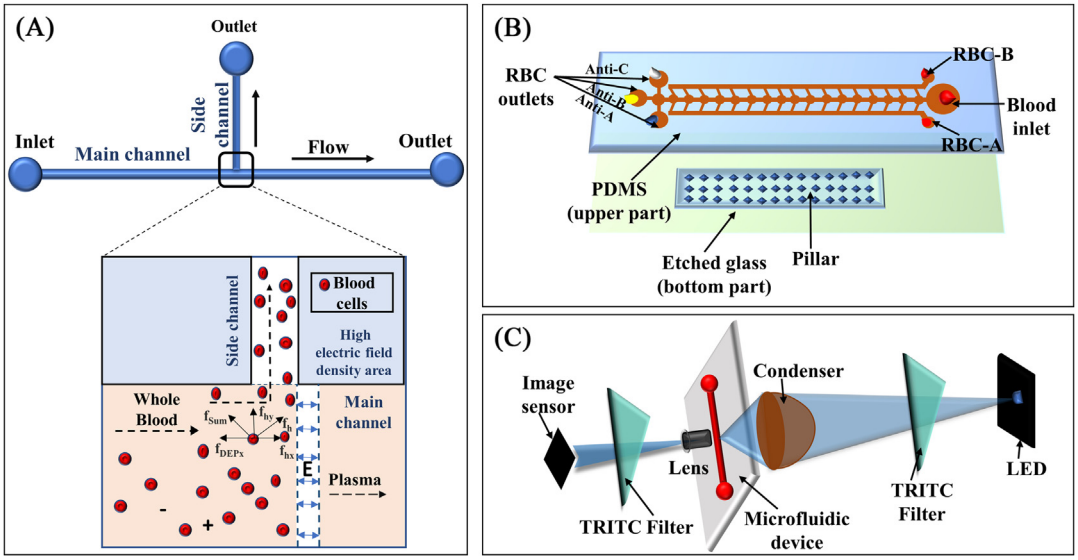

FIGURE 11.2

Schematic presentation of microfluidic chips for on-chip blood analysis and disease diagnosis. (A) A simple dielectrophoresis-based microfluidic device, consisted of a main channel and a side channel with ITO (indium tin oxide) etched two electrodes at the bottom glass surface for blood plasma separation by generating nonuniform electric field, redrawn from Yang, F., Zhang, Y., Cui, X., Fan, Y., Xue, Y., Miao, H. et al. (2019). Extraction of cell-free whole blood plasma using a dielectrophoresis-based microfluidic device. *Biotechnology Journal*, *14*(3), Article e1800181. (B) A passive microfluidic blood typing detector, consisted of a top part and a bottom part. The top part was composed of a fish bone-shaped main channel and two plasma collector channels, while the bottom part was consisted of an array of pillars for RBCs filtration.

Adapted from Karimi, S., Mehrdel, P., Farré-Lladós, J., & Casals-Terré, J. (2019). A passive portable microfluidic blood-plasma separator for simultaneous determination of direct and indirect ABO/Rh blood typing. Lab on a Chip, 19*(19), 3249–3260. (C) An optically modified rectangular shaped microfluidic device for determining the haemoglobin level by measuring the optical density of the samples, redrew from Taparia, N., Platten, K. C., Anderson, K. B., & Sniadecki, N. J. (2017). A microfluidic approach for hemoglobin detection in whole blood.* AIP Advances, 7*(10), 105102.*

multistep diagnostic assay from finger-prick blood collection on a single chip. The blood samples could be loaded directly without any prior processing onto the device by finger prick, making their design accessible for POC diagnosis.

11.2.2 On-chip blood typing

Rapid and accurate blood typing is crucial for blood transfusion, organ transplantation, and any critical medical condition such as pregnancy (Karimi et al., 2019; Zhang et al., 2017). Among more than 30 blood typing methods, ABO/Rh (rhesus) systems attract the most attention due to the high mortality from mismatched ABO/Rh reactions during blood transfusion (Klein et al., 2015; Zhang

et al., 2017). The ABO blood-type is categorized based on the presence or absence of certain antigens (An and B) on the surface of the RBCs (forward typing) and antibodies (anti-An and anti-B) in the plasma (reverse typing) (Karimi et al., 2019; Mujahid & Dickert, 2015), while the Rh type is identified based on the presence (Rh +) or absence (Rh-) of the D antigen in the RBCs (Yamamoto et al., 2020). The basic principle of blood typing relies on the agglutination of the RBCs because of the specific antigen-antibody reaction (Goodell et al., 2010). Forward blood typing is performed by mixing blood cells with the anti-A reagent and anti-B reagent separately. Agglutination of RBCs with the given reagent indicates a positive test result. Agglutination of RBCs with both reagents denotes type AB, while no agglutination, in either case, indicates type O. In reverse grouping, blood plasma is treated against known RBCs from groups An and B (Mujahid & Dickert, 2015). The plasma containing anti-An antibody reacts with the group B RBCs, while anti-B reacts with the group A RBCs and causes agglutination. Agglutination of RBCs, in either case, denotes a positive result. On the other hand, agglutination of RBCs in both cases indicates group O, while no agglutination means group AB. The reverse grouping is mainly done to determine the accuracy of the forward grouping. Similarly, Rh typing is done by adding RBCs with a reagent containing D antibodies. Agglutination of RBCs indicates Rh-positive, while no reaction means Rh-negative (Mujahid & Dickert, 2015). Conventionally blood group is mainly detected using tube test method, slide method, microplate-based method, gel column agglutination, and affinity column technology (Yamamoto et al., 2020) that require special laboratory equipment operated by skilled personnel with long turnaround times (Zhang et al., 2017). Hence, developing simple and cost-effective blood grouping systems is the key demand for facilitating such tools in emergencies and resource-limited areas.

Researchers are aiming to develop LOC-based POC devices for blood typing that could detect both antigens on RBCs (forward) and antibodies from plasma (reverse) from a single drop of blood (Casals-Terré et al., 2020; Chang et al., 2018; Karimi et al., 2019). Zhang et al. (2017) exploited a simple dye-assisted paper-based assay using immobilized antibodies and bromocresol green dye for rapid and reliable detection of ABO/Rh antigens. The device was capable of on-chip blood/plasma separation by capillary action and simultaneous forward-reverse blood grouping within 2 minutes on a single POC chip. The mechanism relies on the visual readout strategy of the reaction between bromocresol green (BCG) and serum protein. The device exhibited teal blue when the blood-type antigens were present and detected the brown color if the antigens were absent. Alongside, passive microfluidic chips in blood-plasma separation become popular because such devices do not require any external energy for fluid movement (Maria et al., 2017). Huet et al. (2018) prepared a passive microfluidic chip with embedded anti-An or anti-B dried reagents inside the microchannel for enhancing capillary flow. The chip provided a rapid and sensitive ABO forward blood typing platform for real-time observation and quantitative measurement of agglutination from a single blood drop with a microscope and a computational unit. Because of the simple operation techniques, only 5 seconds would require to fill the microchannel with the diluted blood sample. It took approximately 2 minutes to generate the data by dissolving the dried reagents in the blood.

Conversely, the working principle of the passive microfluidic devices relies only on capillary forces and may face clogging problems during cell-plasma separation (Karimi et al., 2019; Maria et al., 2017). Karimi et al. (2019) proposed a design by combining a passive microfluidic blood-plasma separator with a blood typing detector for both forward and reverse groupings. Their design allowed the separation of RBCs from plasma by applying hydrodynamic forces through the

generation of stagnation zones, which minimized the clogging of cells and maximized the amount of the extracted plasma in the plasma collector. In fluid dynamics, the stagnation zone is a point in a flow field where the local fluid velocity is zero. The chip consisted of a top part containing a fishbone-shaped main channel with dead-end branches (RBCs outlet) and two plasma collector channels, while the bottom part consisted of an array of diamond-shaped pillars for RBCs filtration and directed the separated plasma towards the plasma collector channel (Fig. 11.2B). The system required only 50 μL of blood without any preanalytical modification. Initially, a droplet of blood was infused into the inlet of the main channel. The plasma was extracted through the arrays of the pillar and collected into the plasma collector channels by capillary forces. Moreover, during this step, the channel geometry allowed the generation of a stagnation zone at the dead-end branches and trapped the RBCs in the RBCs outlets. Specific reagents (anti-A, anti-B, anti-D) for ABO/Rh forward blood typing were added directly into the three RBCs outlets separately for observing agglutination of RBCs. For reverse typing, two known blood samples from Group A and group B were added to the plasma collector separately to observe the possible agglutination of the RBCs. The device achieved a 12% yield of plasma with 100% purity within 10 minutes. The agglutination of RBCs was easily detectable via naked eyes, but the validation was done by analyzing microscopic images to minimize the error. Moreover, to improve the device sensitivity, advanced methods were developed, such as surface plasmon resonance (Szittner et al., 2019; Tangkawsakul et al., 2016) and lab-on-a-disk platform (Chen et al., 2019). In addition, on-chip cross-matching POC tests were carried out by checking the hemocompatibility between the recipient's RBCs and the donor's plasma to prevent the hemolytic transfusion reaction during emergencies (Park & Park, 2018; Yamamoto et al., 2020).

11.2.3 On-chip disease diagnosis

A blood test is considered to be an essential diagnostic tool for monitoring many chronic health conditions. Human blood contains massive information regarding overall health functions. With the rapid technological advancement in LOC, extensive research has been conducted to invent faster and efficient microfluidic POC diagnosis devices for blood diseases. Anemia is perceived as one of the most prevalent blood disorders (Biswas et al., 2018). According to the World Health Organization, approximately a quarter of the world's population is severely affected by anemia (Biswas et al., 2018; Taparia et al., 2017). The causes are related to the fundamental hematologic ailments, iron deficiency, and chronic conditions such as kidney disease, cirrhosis, and infections. This condition is diagnosed by measuring the Hgb concentration in blood. Biswas et al. (2018) reported a simple paper-based colorimetric microfluidic device for POC detection of anemia by measuring the blood Hgb level. This user-friendly microfluidic POC chips comprised 16 circular detection sites, which were separated by a hydrophobic barrier. The colorimetric detection was based on the Hgb catalyzed redox reaction between 3,3′-Dimethyl-[1,1′- biphenyl]-4,4′-diamine (o-tolidine) and hydrogen peroxide, which only cost approximately 0.02$ per test. Heme groups of hemoglobin acts as a chemical catalyst to breakdown the hydrogen peroxide into nascent oxygen and water. Nascent oxygen then oxidizes o-tolidine (Goyal & Basak, 2009). After completing the reaction on the detection side, the color yield was ranging from the lighter shades of bluish-green to deeper-green of oxidized o-tolidine products based on different Hgb levels. The findings were validated by comparing the results from a standard hematology analyzer. This device exhibited

100% specificity with 87.5% and 100% sensitivity for mild and severe anemia successively. Besides, Taparia et al. (2017) developed an optically modified chip to measure the blood Hgb level without cell lysis by measuring the optical density of the samples for different hematocrit levels (Fig. 11.2C). The detection mechanism of Hgb level on their chip was the optical illumination of the samples at 540-nm wavelength and determining the absorbance of the sample by a complementary metal-oxide semiconductor (CMOS) sensor coupled with a lens to magnify the image onto the detector. Another study reported an on-chip quantitative estimation of hematocrit level by measuring the variation of the dielectric/capacitive nature of an erythrocyte cell suspension (Chakraborty et al., 2020). In addition, other groups developed POC diagnostic tool for iron deficiency by using aqueous multiphase systems (Hennek et al., 2016), and molecular fingerprints of Hgb (Saylan & Denizli, 2018) on-chip.

Furthermore, early detection of blood cancer is the prerequisite for successful individualized therapy. Microfluidic LOC techniques become a reliable and affordable platform for isolating different circulating blood cancer cells from the blood of patients in a high-throughput manner (Lee et al., 2018). However, the separation process is still challenging because of the size overlapping between the cancer cells and WBCs. To overcome this challenge, Lee et al. (2018) combined passive hydrodynamic control with phasor-FLIM (fluorescence lifetime imaging microscopy) imaging for label-free size-based cell separation and rapid screening. The device consists of a prefilter region to control the unwanted cell aggregation and a single cell trapping region. Each chip contains 16 identical arrays of highly packed 100 single-cell traps. Because of the height differences between the trapping unit and the main delivery channel, the smaller sized RBCs ran smoothly towards the outlet, but WBCs and leukemia cells were retained into the trapping region. The trapped leukemia cells were easily differentiable from the WBCs in the phasor-FLIM lifetime map based on their significant shift towards the shorter fluorescence lifetime. On-chip lymphoblast isolation was accomplished using affinity separation technique with a purity of approximately 82%−97%, 80%−97%, and 57%−92% for CCRF-CEM lymphoblasts, patient-derived lymphoblast COG-LL332, and COG-LL317 cell lines, respectively (Li et al., 2017). A recent study reported the development of a microfluidic chip for acute promyelocyte leukemia (APL) by the detection of promyelocytic leukemia-retinoic acid receptor α (PML-RARα) fusion protein, which is considered as a diagnostic biomarker in 95% APL cases (Emde et al., 2020). The chip could detect the PML-RARα in cell lysates by a sandwich ELISA (enzyme-linked immunosorbent assay) system on the surface of magnetic streptavidin-coated microparticles within an hour where conventional lab-based techniques require 1−3 days.

Plasma cell disorder, such as multiple myeloma (MM), is responsible for about 20% of death from hematological cancer. The current gold standard for MM detection includes expensive and invasive bone marrow aspiration for detecting clonal plasma cells. However, because of the lower sensitivity and nonuniform distribution of the clonal cells in the bone marrow, this test can produce inaccurate results. On the other hand, studies revealed that some clonal cells leave the bone marrow and entered the peripheral blood of the MM patients (Nowakowski et al., 2005; Ouyang et al., 2019). To isolate and detect clonal cells, microfluidic devices were developed to capture the circulating clonal plasma cells from peripheral blood of the MM patients (Kamande et al., 2018; Ouyang et al., 2019). Ouyang et al. (2019) designed a microfluidic platform to separate circulating clonal plasma cells (cCPC) based on the physical and mechanical properties of the cells. cCPCs possess unique physical and mechanical attributes such as larger size (30−50 μm) (Ouyang et al., 2019)

and high cell membrane elastic modulus (~540 Pa) (Feng et al., 2010) that differentiate them easily from the ordinary blood cells. The device showed approximately 40%−55% capture efficacy from the myeloma cell spiked blood sample. cCPC. Moreover, an affinity selection-based microfluidic chip showed higher sensitivity in cCPC detection among patients with MGUS (monoclonal gammopathy of undetermined significance), smoldering MM, and symptomatic MM (Kamande et al., 2018). Additionally, incorporation of PCR (Polymerase chain reaction) or RT (reverse transcriptase)-PCR technique in microfluidic chips also allows for the detection of genetic blood disorders like thalassemia (Lien et al., 2009) and sickle cell anemia (Zhu, Palla, et al., 2013).

11.3 Smartphone-based platform for blood analysis and disease diagnosis

Smartphone-based biosensor system provides innovative solutions for rapid and accurate on-site qualitative and quantitative POC diagnosis for many diseases (Alawsi & Al-Bawi, 2019; Xu et al., 2018). This widely accessible portable device reduces the size and cost of the laboratory instruments and the professional operation demands (Romeo et al., 2016; Xu et al., 2018). The main advantage of the smartphone-based devices is that the complex sensing system is achievable by integrating additional features such as high-resolution miniature cameras, optical sensors, dongles, and electrical circuits with the in-built mobile sensors for the detection of a wide range of biological signals (Xu et al., 2015, 2018). Moreover, the powerful processor and the smartphone memories make it possible to store the test result, perform on-site data processing and conversion for real-time feedback, and wireless transmission of data to remote sites (Lee et al., 2020; Romeo et al., 2016). Smartphone-based biosensor systems can be categorized according to the analytical method and sensing modality (Xu et al., 2018). Detection via smartphone is generally based on different optical measurements such as bright-field, fluorescence, and/or colorimetric. In this section, we will discuss the widely applied sensing modalities for analyzing blood in smartphone-based LOC devices. Table 11.2 summarizes different smartphone-based devices used in blood analysis.

11.3.1 Microscopic imaging biosensor

Smartphone-based imaging sensors are one of the widely used sensing modalities because of the consistent advancement in the optical imaging hardware of the mobile phone over the past two decades (Ozcan, 2014). By advancing the integrated circuit design and manufacturing technologies, the resolutions of the embedded CMOS image sensor (CIS) cameras in smartphones reach more than 40 MP recently (Ozcan, 2014). Furthermore, by combining different compatible optomechanical attachments with the in-built phone lens and optoelectronic image sensors, the smartphone can be modulated into a microscope. Most smartphone-based microscopes are optical microscopes. A smartphone-based microscope mainly consists of a visible light source and a system of lenses to magnify sample images (Xu et al., 2015). The main purpose of such modification is to develop portable and cost-effective bright-field and fluorescence microscopy for on-site disease diagnosis (Vashist et al., 2014). Also, microscopic images taken with the smartphone can be processed and analyzed easily using simple image recognition software such as ImageJ (Wicks et al., 2017).

Table 11.2 A summary of smartphone-based devices used in blood analysis with various sensing modalities.

Sensing modality	Detect target	Types of smartphone devices	Accessories	Characterization			Application	Accuracy	Reference
				Time	Sample volume	Cost			
Microscopic imaging-Bright-field, Fluorescence	WBCs (white blood cells), RBC (red blood cells), Hemoglobin (Hgb)	Samsung Galaxy SII with 8MPixel color camera and built-in lens with a focal length of f ~4 mm	– A cellphone-based attachment fixed on the top of the cellphone camera unit, worked as battery holder and universal port. – Two AA batteries. – Three separate add-on components for holding the samples. – An inexpensive plano-convex lens for fluorescence imaging. – Light-emitted-diodes (LEDs) for bright-field imaging.	<10 s	~10 μL	–	– Counting of RBC and WBC. – Determining the concentration of Hgb.	In a good agreement with Sysmex KN21 hematology analyzer and the correlation coefficient was ~0.98 and ~0.92 for cell count and Hgb concentration, respectively between the two methods.	Zhu, Sencan, et al. (2013)
Microscopic imaging—Bright-field	RBCs	Nokia N73 camera phones, with a 3.2-megapixel (204861536 pixel) CMOS camera and a 5.664.2 mm sensor, yielding a 2.7 mm pixel spacing.	– A 20× wide field microscope eyepiece (Model NT39−696, Edmunds Optics). – A 0.85 NA 60× Achromat objective (Model NT38−340, Edmunds Optics).	–	A peripheral blood smear was developed by using patient's blood	–	Sickle cell anemia	This system deliberated enough image resolution and contrast for the direct observation of sickled cells in blood smears taken from Hgb SS disease patients with no additional contrast-enhancing techniques.	Breslauer et al. (2009)
Microscopic imaging—Fluorescence	WBCs	Sony-Erickson U10i Aino with ~8 Mpixel color RGB sensor	– A simple lens – A plastic color filter – 3 LEDs – A battery	–	>0.1 mL	Cell phone attachments cost was <14 USD.	Cell density	A decent match was observed between the phone fluorescent images and the conventional fluorescent microscopic images.	Zhu, Yaglidere et al. (2011)
Microscopic imaging—Fluorescence	WBCs	Sony-Erickson U10i Aino with 8 Mpixel color RGB sensor and a built-in lens in front of the CMOS sensor with a focal length of f ~ 4.65 mm.	– A plano-convex lens – A plastic color filter – Two LEDs – Batteries	–	<10 μL	Cell phone attachment cost was <4 USD	Cell density	~95% accuracy against a reference hematology analyzer with a correlation coefficient of ~0.93.	Zhu, Mavandadi, et al. (2011)

(*Continued*)

Table 11.2 A summary of smartphone-based devices used in blood analysis with various sensing modalities. *Continued*

Sensing modality	Detect target	Types of smartphone devices	Accessories	Characterization			Application	Accuracy	Reference
				Time	Sample volume	Cost			
Microscopic imaging—Fluorescence	WBCs	iPhone 8	– A three-layer paper-based microfluidic device for cell sorting. – XFox Professional 300X Optical Glass Lenses – a 500 nm long-pass optical filter – A LED illuminator	5 min	1−4 μL	–	– Sorting of WBCs from whole blood – Quantification of WBCs	∼95% accuracy was noticed compared to the hemocytometer-based manual counting.	Bills et al. (2019)
Optical-intrinsic photothermal response	Hgb	Samsung Galaxy S8 smartphone (Android 8.0.0 operating system), containing a Samsung Exynos 8895 system-on-chip (SoC) with f eight CPU cores.	– Photothermal angular scattering (PTAS) sensor. – A capillary tube for loading blood sample. – Laser diodes (LDs) as probe and PT (photo-therma) excitation light sources. – A circular aperture (700 μm in diameter) was used to control the intensity of probe light. – A complimentary metal-oxide semiconductor (CMOS) sensor for data acquisition and transferring the data to the mobile device for processing.	< 8 s	<150 nL	<0.20 USD for analyzing each sample	Detection of anemia	∼99% accuracy against a reference hematology analyzer with 1.21% of coefficient of variation.	(Lee et al., 2020)
Colorimetric	Hgb	An android phone with AutoCAD 360 app	– A 3D printed point-of-care chip with a rotating ring channel	The auto-mixing of reagents with blood via capillary force was demonstrated within 1 s	∼ 5 μL	Cost per test ∼ 50 cents	Detection of anemia	– The correlation analysis between 3D device and the hematology analyzer gave the coefficient of variation in the range of ∼ 0.2%−5%. – Sensitivity of the test was 81.2% for detecting severe anemia, and 100% for mild anemia.	Plevniak et al. (2016)

								– The diagnostic specificity is 100% for detecting severe anemia, and 83.3% for mild anemia.	
Colorimetric	Hgb	Lenovo S660 (Android version 4.1.2).	– 24 well plate – In-house Hgb calculator app	–	5 μL	Cost per test ~$0.15	Detection of anemia	– The value showed the close agreement to the value achieved from the automated hematology Analyzer with the coefficient of determination of 0.976. – Sensitivity of the test was about 94%. – Specificity of the test was about 90%	Ghatpande et al. (2016)
Colorimetric	RBCs	Galaxy S II, Samsung	– A disposable microfluidic device. – (PDMS) light diffuser. – a PMMA [Poly (methyl methacrylate)] white acrylic box for avoiding variable external light.	–	10 μL	–	Quantification of blood hematocrit	The limit of detection (LOD) obtained from the developed platform was 0.1% of hematocrit with a sensitivity of 0.53 GSV (Gray-scale-valuation) (a.u.)/ hematocrit%	Kim et al. (2017)
Colorimetric	RBCs	Galaxy S II, Samsung	– disposable microfluidic device. – In-house histogram app.	–	10 μL	–	Quantification of blood hematocrit	LOD obtained from the developed platform was 10% of hematocrit	Jalal et al. (2017)
Electrochemical	WBCs	HTC	– Batteries. – A portable potentiostat. – HC-05 Bluetooth Serial – Module. – Power regulator. – Microcontroller.	1 min	10 μL	–	– Leukocytosis – Leukopenia	High repeatability as low as 10% of coefficient of variation.	Wang et al. (2017)

11.3.1.1 Bright-field imaging

Bright-field imaging modality is the simplest optical microscopy modality for POC sensing in smartphone-based devices (Liu et al., 2019; Xu et al., 2018). The primary imaging mechanism of smartphone-based microscopy depends on shadow imaging. Generally, the sample is illuminated uniformly by using a white light source. The light is transmitted through the sample and creates contrasts because of the varied attenuation of the transmitted light in different densities (Drey et al., 2013). Then, CSI camera of the phone captures the images. Zhu, Sencan, et al. (2013) developed a cellphone-based imaging cytometry platform where a 3-part optomechanical system measured the RBCs and WBCs densities and Hgb concentrations (Fig. 11.3A). The device consists of three parts: (1) a cell phone (Samsung Galaxy SII), (2) a cell phone base attachment, which worked as a battery holder and universal port, and (3) three separate add-on sample holders. Samples were placed separately in three different add-on compartments for RBC imaging/counting, WBC imaging/counting, and Hgb concentration measurement. Light-emitting-diodes (LEDs) were used as an illuminator for the bright-field images. For detecting the test value, only approximately 10 μL of the sample was required. A custom-developed application enabled the rapid analysis of the captured microscopic images, which provided the information related to the cell number and Hgb concentration within 10 seconds. For both RBCs and WBCs, the RGB (red, blue, green) values of the acquired images were converted into HS (hue, saturation) values and the maximum intensity contrast between the cells and background was calculated to count the cells. RGB model refers to the biological processing of colors in the human visual system, while HSV (hue, saturation, values) model corresponds to the human perception of the color similarity (Kahu et al., 2019; Loesdau et al., 2014). From HSV images, it is possible to separate the chromatic (hue and saturation) and achromatic (value) information, making it advantageous to measure color information independently from value information (Loesdau et al., 2014). Besides, Hgb concentration was measured by the light transmission intensity of the lysed blood samples. The data for cell counting was comparable with the standard bench-top hematology analyzer (Sysmex KN21), and the correlation coefficient was $\sim$0.98 between the two methods. The Hgb concentration from the cellphone-based system demonstrated a good agreement with that obtained from the Sysmex KN21 hematology analyzer with a correlation coefficient of $\sim$0.92. The data could be stored in the phone memory or transmitted to the central server by a wireless network for remote diagnosis that made this cost-effective blood analyzer advantageous to use in resource-limiting areas.

11.3.1.2 Fluorescence imaging

Smartphone-based fluorescence bioimaging sensor has been widely used because of the simple working principle, high specificity, and strong sensitivity in the detection of the biomarkers (Arts et al., 2016; Priye et al., 2017; Xu et al., 2018). The optomechanical modification of such devices is different from the bright-field imaging technique. Smartphone-based fluorescence microscope generally contains an excitation, and an emission filter, and an excitation source such as laser diodes (Xu et al., 2018). A simple, cost-effective cellphone-based fluorescence microscopic platform was developed for wide-field imaging and rapid quantification of fluorescently labeled biomarkers using a small blood volume (Zhu, Yaglidere, et al., 2011). The existing cellphone camera was modified by compact and light-weighted (28 g) attachments, including 3 LEDs, a simple lens, and a mechanical holder for the plastic color filter for achieving 10 mm resolution across

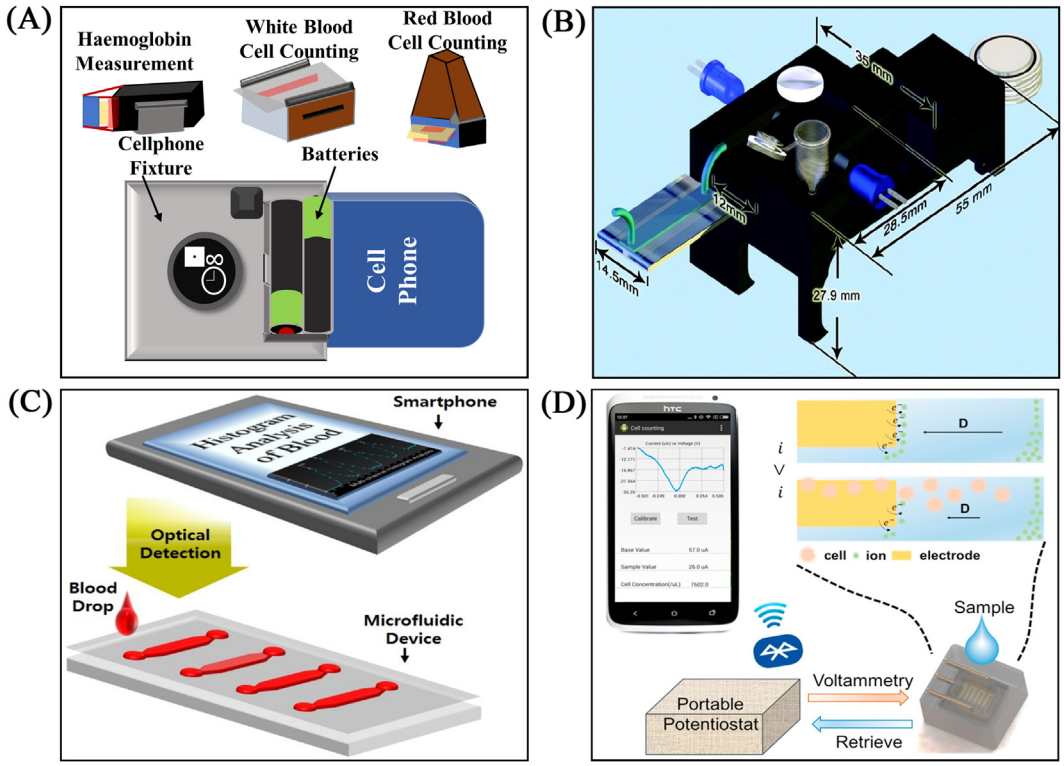

FIGURE 11.3

Examples of smartphone-based bioimaging sensors. (A) A bright-field imaging sensor for counting blood cells and measuring hemoglobin concentration.

Adapted from Zhu, H., Sencan, I., Wong, J., Dimitrov, S., Tseng, D., Nagashima, K. et al. (2013). Cost-effective and rapid blood analysis on a cell-phone. Lab on a Chip, 13*(7), 1282–1288. (B) A wide-field fluorescent imaging sensor on the smartphone for blood cells counting, adapted from Zhu, H., Mavandadi, S., Coskun, A. F., Yaglidere, O., & Ozcan, A. (2011). Optofluidic fluorescent imaging cytometry on a cell phone.* Analytical Chemistry, 83*(17), 6641–6647. (C) A colorimetric optical sensor for determining blood haematocrit, adapted from Jalal, U. M., Kim, S. C., & Shim, J. S. (2017). Histogram analysis for smartphone-based rapid hematocrit determination.* Biomedical Optical Express, 8*(7), 3317–3328. (D) An electrochemical counter for label-free counting of white blood cells, adapted from Wang, X., Lin, G., Cui, G., Zhou, X., & Liu, G. L. (2017). White blood cell counting on smartphone paper electrochemical sensor.* Biosensors and Bioelectronics, 90, *549–557.*

a field-of-view of 81 mm^2. The main advantage of this design was the changeable LEDs and the plastic filter for different excitation/emission wavelengths that made the device suitable for a wide range of fluorophores. The device feasibility was investigated by detecting the fluorescently labeled WBCs from whole blood samples. The WBCs were labeled with STYO16 nucleic acid staining and excited with blue LEDs at 470 nm peak wavelength. The images were taken by the phone camera and compared to that taken by the conventional fluorescent microscope. The number of the cells showed a decent match in both methods that suggested the usefulness of the device for wide-field

imaging and quantification in the resource-limited settings. The same group developed another optofluidic imaging cytometry platform for detecting fluorescently labeled WBCs (Fig. 11.3B) (Zhu, Mavandadi, et al., 2011). The main difference of this device from the previous design was the use of disposable microfluidic channels for the continuous flow of the samples with a syringe pump at the flow rate of $\sim 1\ \mu L$/minute for 5−6 minutes. The team also reduced the manufacturing cost by approximately US$ 10 and the sample volume (~ 10 times lower) than the old design. Moreover, the imaging resolution of the device was improved up to $\sim 2\ \mu m$ in fluorescent imaging mode by using a plano-convex lens with a focal length of ~ 0.6 mm. The microfluidic device was placed above the phone camera and also coupled with the cheap LEDs to use as a multilayered optofluidic waveguide for the sample excitation. The microscopic fluorescence movie of the cells was taken by the phone camera. The rapid digital photo processing was done by using the contour detection algorithm. The system was able to count the labeled cells automatically. The results obtained from the device matched well with the standard hematology analyzer with 95% accuracy.

11.3.2 Colorimetric detection

Colorimetric optical sensing is the most commonly used technique in smartphone-based POC diagnosis, where an ambient light sensor collects the photons from the sample directly and then capture the images by using the phone camera (Dutta, 2019; Liu et al., 2019). A simple smartphone-based colorimetric test mainly requires illumination and image processing with the in-built CMOS image sensor (Liu et al., 2019). This test detects the concentration of biomarkers in the sample with the help of the color reagent, based on the absorbance or reflected intensity differences of the biomarker-reagent complexes (Heo et al., 2014). Plevniak et al. (2016) reported a smartphone integrated 3D microfluidic auto-mixing device that can perform colorimetric quantification of Hgb level. The unique design of the device with a rotating ring channel enabled the rapid mixing of the blood and oxidizing agent inside the device within a second by capillary force. An in-house written color-scale analytical app with the smartphone output app (AutoCAD 360) was used for the colorimetric detection of blood Hgb. The visual readout was depending on the oxidation−reduction reaction in the blood Hgb and oxidizing agent. With increased Hgb concentration, the visual representation of the tested samples presented in a color span blue, green, yellow, orange, and red. The photospectrometer measurements calibrated the visual data for quantitative measurement of Hgb concentrations. The device is suitable for the color-blind patients. Besides the low cost, this colorimetric based microfluidic device showed almost 100% specificity for detecting severe anemia, while 83.3% for mild anemia. Another smartphone-based application was developed for the accurate and sensitive colorimetric measurement of blood Hgb level by Ghatpande et al. (2016). The colorimetric estimation was measured using an in-house app, named Hb calculator, operated by a Lenovo S660 (Android version 4.1.2). The mobile phone app converted the variation of color intensity into digitalized values to estimate the Hgb concentration. This simple device only used 5 μL of blood for analysis and showed approximately 94% specificity with 90% sensitivity in Hgb detection.

Moreover, Kim et al. (2017) directly used the intrinsic programs of the smartphone for analyzing blood hematocrit and imaging. A specialized optical setup, including an optical diffuser and a reflector, was used to avoid the image burning via the smartphone flashlight and the ambient light effect during picture collection. The results showed a linear increase of GSV (Gray-scale-valuation)

value with the raising hematocrit concentration of the sample. The same group later proposed another smartphone-based microfluidic chip for rapid detection and quantification of blood hematocrit by an in-house "Histogram" app (Fig. 11.3C) (Jalal et al., 2017). The main advantage of the later design was the integration of a software-based histogram algorithm instead of the hardware modification. The integrated "Histogram" app could automatically detect the blood samples in the microfluidic channels and quantify the blood hematocrit in equal and varying optical conditions with auto-calibration. However, the limit of detection (LOD) obtained from the previous design was 0.1% of hematocrit, while the later one needed at least 10% of hematocrit present in the sample.

11.3.3 Electrochemical biosensing

An electrochemical-based sensing system works by transferring the electrochemical information into an analytically useful signal. In an electrochemical sensing system, two components including a chemical (molecular) recognition system and a physicochemical transducer for signal detection, are required to form a sensing electrode (Faridbod et al., 2011). POC devices with an electrochemical sensor are widely used in medical testing and analytical chemistry because of the high precision, rapid responses, cost-efficacy, and portability (Yu, Zhang, Buscaglia, et al., 2016; Yu, Zhang, Chang, et al., 2016; Zhang et al., 2018). A smartphone-based electrochemical counter was proposed by Wang et al. (2017) for label-free WBC counting (Fig. 11.3D). The device was based on microporous paper with gold microelectrodes. When the cells were trapped on the membrane and covered the microelectrodes, the voltammetry signal was generated from a portable potentiostat. Simultaneously, the received signal was retrieved and transmitted to the smartphone through the Bluetooth module. A smartphone app analyzed the signals and evaluated the cell concentration value within a minute. The system could quantify the cell concentration, covering from physiological to the pathological range, by using only 10 μL of blood.

11.4 Conclusion and perspective

Microfluidic LOC devices are bridging the gap between the laboratory centralized blood test and POC platform for the early detection of diseases. LOC devices reduce the sample volume on a micrometer scale and minimizes the data acquisition time. Combining smartphone-based sensing technology with LOC drastically cuts down the per-test cost to less than a dollar with high accuracy and sensitivity. Though there are significant research efforts to develop simple, low cost, portable POC devices, the commercialization of such devices remains restricted. Scalability is an important requirement for commercialization, where complex device structures create challenges. Introducing 3D printing in device fabrication instead of lithographic techniques proves beneficial in case of scalability. Meanwhile, most LOC devices are not fully automatic and require external equipment for sample handling and preparation. Moreover, data acquisition and processing also need expensive instruments such as microscopes and computational units. Besides, smartphone-based devices use in-house programs that are not available for mass application. Researchers should consider using the in-built smartphone Apps or design user-friendly programs for translating data

into a simple visual readout. Smartphone-based devices can cause potential contamination because of poor hygiene control. Automation of all assay steps such as sample and reagent integration, mixing, separation, washing, and data acquisition might minimize the error and contamination. To achieve this aim, researchers can consider installing simple reagent storage and micropump for automatic handling without manual intervention. For disease diagnosis, most studies used spiked samples by adding a known quantity of cells of interest, such as tumor cells with the blood that made it challenging to translate the test results into the clinical setup. Clinical samples directly collected from the patients should be analyzed instead of spiked samples to validate the integrity of the devices. Finally, multiplexing, or simultaneous detection of different blood analytes is still not possible by LOC devices. In the future, scientists should make significant efforts to develop a multiplex POC platform from complete blood analysis to disease diagnosis.

Abbreviations

CMOS Complementary metal-oxide-semiconductor
cCPC Circulating clonal plasma cell
CIS CMOS image sensor
Hgb Hemoglobin
LEDs Light-emitting-diodes
LOC Lab-on-a-chip
MM Multiple myeloma
PBS Phosphate buffer saline
PDMS Polydimethylsiloxane,
POC Point-of-care
RBCs Red blood cells
Rh Rhesus
WBCs White blood cells

References

Alawsi, T., & Al-Bawi, Z. (2019). A review of smartphone point-of-care adapter design. *Engineering Reports*, *1*(2), e12039.

Arshavsky-Graham, S., & Segal, E. (2020) *Lab-on-a-chip devices for point-of-care medical diagnostics* (pp. 1−19). In: Advances in Biochemical Engineering/Biotechnology. Berlin, Heidelberg: Springer. Available from: https://doi.org/10.1007/10_2020_127

Arts, R., den Hartog, I., Zijlema, S. E., Thijssen, V., van der Beelen, S. H. E., & Merkx, M. (2016). Detection of antibodies in blood plasma using bioluminescent sensor proteins and a smartphone. *Analytical Chemistry*, *88*(8), 4525−4532.

Bills, M. V., Nguyen, B. T., & Yoon, J.-Y. (2019). Simplified white blood cell differential: An inexpensive, smartphone- and paper-based blood cell count. *IEEE Sensors Journal*, *19*(18), 7822−7828.

Biswas, S. K., Bandyopadhyay, S., Kar, S., Som, N. K., & Chakraborty, S. (2018). Anemia diagnosis on a simple paper-based assay. *bioRxiv*, 439224.

Breslauer, D. N., Maamari, R. N., Switz, N. A., Lam, W. A., & Fletcher, D. A. (2009). Mobile phone based clinical microscopy for global health applications. *PLoS One*, *4*(7), e6320.

Casals-Terré, J., Farré-Lladós, J., López, J. A., Vidal, T., & Roncero, M. B. (2020). Enhanced fully cellulose based forward and reverse blood typing assay. *Journal of Biomedical Materials Research. Part B, Applied Biomaterials*, *108*(2), 439−450.

Chakraborty, S., Das, S., Das, C., Chandra, S., Sharma, K. D., Karmakar, A., et al. (2020). On-chip estimation of hematocrit level for diagnosing anemic conditions by Impedimetric techniques. *Biomedical Microdevices*, *22*(2), 38.

Chang, Y. J., Fan, Y. H., Chen, S. C., Lee, K. H., & Lou, L. Y. (2018). An automatic lab-on-disc system for blood typing. *SLAS Technology*, *23*(2), 172−178.

Chen, J.-Y., Huang, Y.-T., Chou, H.-H., Wang, C.-P., & Chen, C.-F. (2015). Rapid and inexpensive blood typing on thermoplastic chips. *Lab on a Chip*, *15*(24), 4533−4541.

Chen, Y.-W., Li, W.-T., Chang, Y., Lee, R.-H., & Hsiue, G.-H. (2019). Blood-typing and irregular antibody screening through multi-channel microfluidic discs with surface antifouling modification. *Biomicrofluidics.*, *13*(3), 034107.

Dixon, C., Lamanna, J., & Wheeler, A. R. (2020). Direct loading of blood for plasma separation and diagnostic assays on a digital microfluidic device. *Lab on a Chip*, *20*(10), 1845−1855.

Drey, L. L., Graber, M. C., & Bieschke, J. (2013). Counting unstained, confluent cells by modified bright-field microscopy. *Biotechniques*, *55*(1), 28−33.

Dutta, S. (2019). Point of care sensing and biosensing using ambient light sensor of smartphone: Critical review. *TrAC Trends in Analytical Chemistry*, *110*, 393−400.

Emde, B., Kreher, H., Bäumer, N., Bäumer, S., Bouwes, D., & Tickenbrock, L. (2020). Microfluidic-based detection of AML-specific biomarkers using the example of promyelocyte leukemia. *International Journal of Molecular Science*, *21*(23).

Faridbod, F., Gupta, V. K., & Zamani, H. A. (2011). Electrochemical sensors and biosensors. *International Journal of Electrochemistry*, *2011*, 352546.

Feng, Y., Ofek, G., Choi, D. S., Wen, J., Hu, J., Zhao, H., et al. (2010). Unique biomechanical interactions between myeloma cells and bone marrow stroma cells. *Progress in Biophysics and Molecular Biology*, *103*(1), 148−156.

Ghatpande, N. S., Apte, P. P., Joshi, B. N., Naik, S. S., Bodas, D., Sande, V., et al. (2016). Development of a novel smartphone-based application for accurate and sensitive on-field hemoglobin measurement. *RSC Advances*, *6*(106), 104067−104072.

Goodell, P. P., Uhl, L., Mohammed, M., & Powers, A. A. (2010). Risk of hemolytic transfusion reactions following emergency-release RBC transfusion. *American Journal of Clinical Pathology*, *134*(2), 202−206.

Goyal, M. M., & Basak, A. (2009). Estimation of plasma haemoglobin by a modified kinetic method using o-tolidine. *Indian Journal of Clinical Biochemistry*, *24*(1), 36−41.

Hennek, J. W., Kumar, A. A., Wiltschko, A. B., Patton, M. R., Lee, S. Y., Brugnara, C., et al. (2016). Diagnosis of iron deficiency anemia using density-based fractionation of red blood cells. *Lab on a Chip*, *16*(20), 3929−3939.

Heo, J. H., Cho, H. H., Lee, J. W., & Lee, J. H. (2014). Achromatic−chromatic colorimetric sensors for on−-off type detection of analytes. *Analyst.*, *139*(24), 6486−6493.

Huet, M., Cubizolles, M., & Buhot, A. (2017). Real time observation and automated measurement of red blood cells agglutination inside a passive microfluidic biochip containing embedded reagents. *Biosensors & Bioelectronics*, *93*, 110−117.

Huet, M., Cubizolles, M., & Buhot, A. (2018). Red blood cell agglutination for blood typing within passive microfluidic biochips. *High Throughput*, *7*(2).

Jalal, U. M., Kim, S. C., & Shim, J. S. (2017). Histogram analysis for smartphone-based rapid hematocrit determination. *Biomedical Optical Express*, *8*(7), 3317−3328.

Kahu, S. Y., Raut, R. B., & Bhurchandi, K. M. (2019). Review and evaluation of color spaces for image/video compression. *Color Research & Application*, *44*(1), 8−33.

Kamande, J. W., Lindell, M. A. M., Witek, M. A., Voorhees, P. M., & Soper, S. A. (2018). Isolation of circulating plasma cells from blood of patients diagnosed with clonal plasma cell disorders using cell selection microfluidics. *Integrative Biology*, *10*(2), 82−91.

Karimi, S., Mehrdel, P., Farré-Lladós, J., & Casals-Terré, J. (2019). A passive portable microfluidic blood−plasma separator for simultaneous determination of direct and indirect ABO/Rh blood typing. *Lab on a Chip*, *19*(19), 3249−3260.

Kersaudy-Kerhoas, M., & Sollier, E. (2013). Micro-scale blood plasma separation: From acoustophoresis to egg-beaters. *Lab on a Chip*, *13*(17), 3323−3346.

Kim, B. J., Lee, Y. S., Zhbanov, A., & Yang, S. (2019). A physiometer for simultaneous measurement of whole blood viscosity and its determinants: Hematocrit and red blood cell deformability. *Analyst.*, *144*(9), 3144−3157.

Kim, S. C., Jalal, U. M., Im, S. B., Ko, S., & Shim, J. S. (2017). A smartphone-based optical platform for colorimetric analysis of microfluidic device. *Sensors and Actuators B: Chemical*, *239*, 52−59.

Klein, H. G., Cortés-Puch, I., & Natanson, C. (2015). Blood-transfusion decisions not simple. *Nature*, *521* (7552), 289.

Kuan, D.-H., & Huang, N.-T. (2020). Recent advancements in microfluidics that integrate electrical sensors for whole blood analysis. *Analytical Methods*, *12*(26), 3318−3332.

Kuan, D. H., Wang, I. S., Lin, J. R., Yang, C. H., Huang, C. H., Lin, Y. H., et al. (2016). A microfluidic device integrating dual CMOS polysilicon nanowire sensors for on-chip whole blood processing and simultaneous detection of multiple analytes. *Lab on a Chip*, *16*(16), 3105−3113.

Kuan, D. H., Wu, C. C., Su, W. Y., & Huang, N. T. (2018). A microfluidic device for simultaneous extraction of plasma, red blood cells, and on-chip white blood cell trapping. *Science Reports*, *8*(1), 15345.

Lee, D. H., Li, X., Ma, N., Digman, M. A., & Lee, A. P. (2018). Rapid and label-free identification of single leukemia cells from blood in a high-density microfluidic trapping array by fluorescence lifetime imaging microscopy. *Lab on a Chip*, *18*(9), 1349−1358.

Lee, J., & Lee, S.-H. (2013). Lab on a chip for in situ diagnosis: From blood to point of care. *Biomedical Engineering Letters*, *3*(2), 59−66.

Lee, J., Song, J., Choi, J.-H., Kim, S., Kim, U., Nguyen, V.-T., et al. (2020). A portable smartphone-linked device for direct, rapid and chemical-free hemoglobin assay. *Scientific Reports*, *10*(1), 8606.

Lee, K. K., Kim, M. O., & Choi, S. (2019). A whole blood sample-to-answer polymer lab-on-a-chip with superhydrophilic surface toward point-of-care technology. *Journal of Pharmaceutical and Biomedical Analysis*, *162*, 28−33.

Microfluidics in lab-on-a-chip: Models, simulations and experiments. In D. Li (Ed.), *Microscale heat transfer fundamentals and applications*. Dordrecht, Netherlands: Springer.

Li, T., Fan, Y., Cheng, Y., & Yang, J. (2013). An electrochemical Lab-on-a-CD system for parallel whole blood analysis. *Lab on a Chip*, *13*(13), 2634−2640.

Li, W., Zhang, Y., Reynolds, C. P., & Pappas, D. (2017). Microfluidic separation of lymphoblasts for the isolation of acute lymphoblastic leukemia using the human transferrin receptor as a capture target. *Analytical Chemistry*, *89*(14), 7340−7347.

Lien, K. Y., Liu, C. J., Kuo, P. L., & Lee, G. B. (2009). Microfluidic system for detection of alpha-thalassemia-1 deletion using saliva samples. *Analytical Chemistry*, *81*(11), 4502−4509.

Liu, J., Geng, Z., Fan, Z., Liu, J., & Chen, H. (2019). Point-of-care testing based on smartphone: The current state-of-the-art (2017−2018). *Biosensors and Bioelectronics*, *132*, 17−37.

Hue and saturation in the RGB color space. In M. Loesdau, S. Chabrier, & A. Gabillon (Eds.), *Image and signal processing*. Cham: Springer International Publishing.

Mabey, D., Peeling, R. W., Ustianowski, A., & Perkins, M. D. (2004). Diagnostics for the developing world. *Nature Reviews: Microbiology*, *2*(3), 231−240.

Mach, A. J., Adeyiga, O. B., & Di Carlo, D. (2013). Microfluidic sample preparation for diagnostic cytopathology. *Lab on a Chip*, *13*(6), 1011−1026.
Madadi, H., Casals-Terré, J., & Mohammadi, M. (2015). Self-driven filter-based blood plasma separator microfluidic chip for point-of-care testing. *Biofabrication.*, *7*(2), 025007.
Mantegazza, A., Clavica, F., & Obrist, D. (2020). In vitro investigations of red blood cell phase separation in a complex microchannel network. *Biomicrofluidics.*, *14*(1), 014101.
Maria, M. S., Chandra, T. S., & Sen, A. K. (2017). Capillary flow-driven blood plasma separation and on-chip analyte detection in microfluidic devices. *Microfluid Nanofluidics*, *21*(4), 72.
Mujahid, A., & Dickert, F. L. (2015). Blood group typing: From classical strategies to the application of synthetic antibodies generated by molecular imprinting. *Sensors*, *16*(1), 51, Basel.
Nguyen, J., Wei, Y., Zheng, Y., Wang, C., & Sun, Y. (2015). On-chip sample preparation for complete blood count from raw blood. *Lab on a Chip*, *15*(6), 1533−1544.
Nikoleli, G.-P., Siontorou, C. G., Nikolelis, D. P., Bratakou, S., Karapetis, S., & Tzamtzis, N. (2018). Chapter 13—Biosensors based on microfluidic devices lab-on-a-chip and microfluidic technology. In D. P. Nikolelis, & G.-P. Nikoleli (Eds.), *Nanotechnology and biosensors* (pp. 375−394). Elsevier.
Nowakowski, G. S., Witzig, T. E., Dingli, D., Tracz, M. J., Gertz, M. A., Lacy, M. Q., et al. (2005). Circulating plasma cells detected by flow cytometry as a predictor of survival in 302 patients with newly diagnosed multiple myeloma. *Blood*, *106*(7), 2276−2279.
Ouyang, D., Li, Y., He, W., Lin, W., Hu, L., Wang, C., et al. (2019). Mechanical segregation and capturing of clonal circulating plasma cells in multiple myeloma using micropillar-integrated microfluidic device. *Biomicrofluidics.*, *13*(6), 064114.
Ozcan, A. (2014). Mobile phones democratize and cultivate next-generation imaging, diagnostics and measurement tools. *Lab on a Chip*, *14*(17), 3187−3194.
Park, J., & Park, J. K. (2018). Finger-actuated microfluidic device for the blood cross-matching test. *Lab on a Chip*, *18*(8), 1215−1222.
Plevniak, K., Campbell, M., & Mei, H. (2016). 3D printed microfluidic mixer for point-of-care diagnosis of anemia. *Annual International Conference on IEEE Engineering, Medical and Biological Society*, *2016*, 267−270.
Priye, A., Bird, S. W., Light, Y. K., Ball, C. S., Negrete, O. A., & Meagher, R. J. (2017). A smartphone-based diagnostic platform for rapid detection of Zika, chikungunya, and dengue viruses. *Scientific Reports*, *7*, 44778.
Romeo, A., Leung, T. S., & Sánchez, S. (2016). Smart biosensors for multiplexed and fully integrated point-of-care diagnostics. *Lab on a Chip*, *16*(11), 1957−1961.
Saylan, Y., & Denizli, A. (2018). Molecular fingerprints of hemoglobin on a nanofilm chip. *Sensors*, *18*(9), Basel.
Szittner, Z., Bentlage, A. E. H., van der Donk, E., Ligthart, P. C., Lissenberg-Thunnissen, S., van der Schoot, C. E., et al. (2019). Multiplex blood group typing by cellular surface plasmon resonance imaging. *Transfusion*, *59*(2), 754−761.
Tangkawsakul, W., Srikhirin, T., Shinbo, K., Kato, K., Kaneko, F., & Baba, A. (2016). Application of long-range surface plasmon resonance for ABO blood typing. *International Journal of Analytical Chemistry*, *2016*, 1432781.
Taparia, N., Platten, K. C., Anderson, K. B., & Sniadecki, N. J. (2017). A microfluidic approach for hemoglobin detection in whole blood. *AIP Advances*, *7*(10), 105102.
Vashist, S. K., Mudanyali, O., Schneider, E. M., Zengerle, R., & Ozcan, A. (2014). Cellphone-based devices for bioanalytical sciences. *Analytical and Bioanalytical Chemistry*, *406*(14), 3263−3277.
Wang, X., Lin, G., Cui, G., Zhou, X., & Liu, G. L. (2017). White blood cell counting on smartphone paper electrochemical sensor. *Biosensors and Bioelectronics*, *90*, 549−557.

Wicks, L. C., Cairns, G. S., Melnyk, J., Bryce, S., Duncan, R. R., & Dalgarno, P. A. (2017). EnLightenment: High resolution smartphone microscopy as an educational and public engagement platform. *Wellcome Open Research*, *2*, 107.

Xu, D., Huang, X., Guo, J., & Ma, X. (2018). Automatic smartphone-based microfluidic biosensor system at the point of care. *Biosensors and Bioelectronics*, *110*, 78–88.

Xu, X., Akay, A., Wei, H., Wang, S., Pingguan-Murphy, B., Erlandsson, B., et al. (2015). Advances in smartphone-based point-of-care diagnostics. *Proceedings of the IEEE*, *103*(2), 236–247.

Yamamoto, K., Sakurai, R., & Motosuke, M. (2020). Fully-automatic blood-typing chip exploiting bubbles for quick dilution and detection. *Biomicrofluidics.*, *14*(2), 024111.

Yang, F., Zhang, Y., Cui, X., Fan, Y., Xue, Y., Miao, H., et al. (2019). Extraction of cell-free whole blood plasma using a dielectrophoresis-based microfluidic device. *Biotechnology Journal*, *14*(3), e1800181.

Yu, Y., Zhang, Q., Buscaglia, J., Chang, C.-C., Liu, Y., Yang, Z., et al. (2016). Quantitative real-time detection of carcinoembryonic antigen (CEA) from pancreatic cyst fluid using 3-D surface molecular imprinting. *Analyst.*, *141*(14), 4424–4431.

Yu, Y., Zhang, Q., Chang, C.-C., Liu, Y., Yang, Z., Guo, Y., et al. (2016). Design of a molecular imprinting biosensor with multi-scale roughness for detection across a broad spectrum of biomolecules. *Analyst.*, *141*(19), 5607–5617.

Zhang, H., Qiu, X., Zou, Y., Ye, Y., Qi, C., Zou, L., et al. (2017). A dye-assisted paper-based point-of-care assay for fast and reliable blood grouping. *Science Translational Medicine*, *9*(381).

Zhang, Q., Kaisti, M., Prabhu, A., Yu, Y., Song, Y.-A., Rafailovich, M. H., et al. (2018). Polyaniline-functionalized ion-sensitive floating-gate FETs for the on-chip monitoring of peroxidase-catalyzed redox reactions. *Electrochimica Acta*, *261*, 256–264.

Zhu, H., Mavandadi, S., Coskun, A. F., Yaglidere, O., & Ozcan, A. (2011). Optofluidic fluorescent imaging cytometry on a cell phone. *Analytical Chemistry*, *83*(17), 6641–6647.

Zhu, H., Sencan, I., Wong, J., Dimitrov, S., Tseng, D., Nagashima, K., et al. (2013). Cost-effective and rapid blood analysis on a cell-phone. *Lab on a Chip*, *13*(7), 1282–1288.

Zhu, H., Yaglidere, O., Su, T. W., Tseng, D., & Ozcan, A. (2011). Cost-effective and compact wide-field fluorescent imaging on a cell-phone. *Lab on a Chip*, *11*(2), 315–322.

Zhu, J., Palla, M., Ronca, S., Warpner, R., Ju, J., & Lin, Q. (2013). A MEMS-based approach to single nucleotide polymorphism genotyping. *Sensors and Actuators. A, Physical*, *195*, 175–182.